Chapter 5

Stability Analysis of Nonlinear Discrete-Time Adaptive Control Systems with Large Dead-Times - Theory and a Case Study

Mario A. Jordan, Jorge L. Bustamante and
Carlos E. Berger

Additional information is available at the end of the chapter

http://dx.doi.org/10.5772/52224

1. Introduction

Accordingly to modern digital technology in control communications and optic fiber, unmanned underwater vehicles (UUV) are usually controlled digitally. In the case of remotely operated vehicles (ROV), partial control systems are useful, for instance for the roll-pitch stabilization, as long as the main modes of motion are performed basically by teleoperation. In the case of autonomous underwater vehicles (AUV) on the contrary, the control of modes is complete, it means, the advance, the immersion and the roll-pitch stabilization are carried out automatically with a large degree of self-decision both in guidance and control.

In all cases, digital communications between the controller, the guide system and the navigation system are often affected by a pure delay in the control action, which correctively manipulates the vehicle behavior with lateness through their thrusters. Generally speaking, the delay is variable because of the commonly sophisticated nature of protocols involved in the usual communication standards, for instance in the well-widespread protocols RS422/485. In many cases, the delay problem is much more complex and embraces a pure delay for the sensor instruments and other quite different ones for the controller and guidance communications. Moreover, sensors may have different delays each one, due to different hardware and baud rates in data transmission.

Pure delays can influence significantly the stability of UUV's, principally in fast motions like in the modes of pitch and roll, causing, in extreme fall, the capsize of the vehicle. Additionally, the well-known strong interaction among the modes in the dynamics of UUV's may cause large oscillations of the pitch modes that are induced by acelerations in the advance mode. Thus, complex control systems for the whole 6-degrees-of freedom (DOF) dynamics are much more preferable than many single-mode controllers.

Dealing with pure delays in the controller design, a Smith-predictor solution stays in mind at the first place. However, the needs of a precise model to construct the predictor upon the usually uncertain and potentially unstable dynamics of an UUV, makes this alternative quite unfeasible (Leonard and Abba, 2012). On the other way, simple controllers like for instance PID controllers, are viable to be tuned with less dynamics information but generally can not counteract by itself the undesirable effects of relatively large pure delays. Adaptive controllers had proved to work properly in these scenarios with many advantages (Jordán and Bustamante, 2011). Nevertheless, the roll played by pure delays in the stability and performance of control systems for underwater vehicles is much less dealt with in the specialized literature.

In this Chapter we focus the design of a 6-degrees-of-freedom adaptive controller for UUV's directly in the sample-time domain. The controller pertains to the class of speed gradient adaptive control systems. This controller was developed in (Jordán and Bustamante, 2011) and shows clearly advantages in stability over the same digital speed-gradient controller which is first designed in continuous time and finally translated to discrete time. One starts from the fact that the UUV dynamics, together with the control communication link in the feedback, involves a considerable delay. In this work, we depart from a hypothesis that an optimal sampling time for the control stability should have some upper limit for the stability in the presence of pure delays, disturbances in the samples and rapid desired maneuvers. To support our hypothesis, we close the analysis with a classification of certain influence variables on the stability and performance of the proposed digital adaptive control system.

2. UUV dynamics

Let $\boldsymbol{\eta}=[x,y,z,\varphi,\theta,\psi]^T$ be the generalized position vector of the UUV referred to an earth-fixed coordinate system termed O', with displacements x,y,z, and rotation angles φ,θ,ψ about these directions, respectively. The motions associated to the elements of $\boldsymbol{\eta}$ are referred to as surge, sway, heave, roll, pitch and yaw, respectively.

Additionally let $\boldsymbol{v}=[u,v,w,p,q,r]^T$ be the generalized rate vector referred on a vehicle-fixed coordinate system termed O, oriented according to its main axes with translation rates u,v,w and angular rates p,q,r about these directions, respectively.

The vehicle dynamics with a time delay in the communication system, is described by the ODE (*cf.* Jordán and Bustamante, 2009a; *cf.* Fossen, 1994)

$$\dot{\boldsymbol{v}}=M^{-1}\left(-C[\boldsymbol{v}]\boldsymbol{v}-D[|\boldsymbol{v}|]\boldsymbol{v}-\boldsymbol{g}[\boldsymbol{\eta}]+\boldsymbol{\tau}_c+\boldsymbol{\tau}(t-T_d)\right) \tag{1}$$

$$\dot{\boldsymbol{\eta}}=J[\boldsymbol{\eta}](\boldsymbol{v}+\boldsymbol{v}_c). \tag{2}$$

Here M, C and D are the inertia, the Coriolis-centripetal and the drag matrices, respectively and J is the matrix expressing the transformation from the inertial frame to the vehicle-fixed frame. Moreover, $\boldsymbol{g}$ is the restoration force due to buoyancy and weight, $\boldsymbol{\tau}$ is the generalized propulsion force whose action is delayed T_d seconds, $\boldsymbol{\tau}_c$ is a generalized perturbation force (for instance due to cable tugs in ROV's) and $\boldsymbol{v}_c$ is a velocity perturbation (for instance the fluid current in ROV's/AUV's), all of them applied to O.

http://dx.doi.org/10.5772/52224

From now on, brackets are employed to indicate functional dependence and parenthesis to denote common factor. Besides vectors are indicated in bold, variables in italics and matrices in capital letters.

Notice from (1) the nonlinear dependence of C, D and $\boldsymbol{g}$ with the states $\boldsymbol{v}$ and $\boldsymbol{\eta}$.

Moreover, we will concentrate henceforth on disturbed measures $\boldsymbol{\eta}_\delta$ and $\boldsymbol{v}_\delta$, and not on exogenous perturbations $\boldsymbol{\tau}_c$ and $\boldsymbol{v}_c$, so we have set $\boldsymbol{\tau}_c$=$\boldsymbol{v}_c$=0 throughout the Chapter. For more explanations about the influence of $\boldsymbol{\tau}_c$ and $\boldsymbol{v}_c$ on adaptive guidance systems see (Jordán and Bustamante, 2008; Jordán and Bustamante 2007), respectively.

3. Sampled-data behavior

For the continuous-time dynamics there exists an associated exact sampled-data dynamics described by the set of sequences $\{\boldsymbol{\eta}[t_i], \boldsymbol{v}[t_i]\} = \{\boldsymbol{\eta}_{t_i}, \boldsymbol{v}_{t_i}\}$ for the states $\boldsymbol{\eta}[t]$ and $\boldsymbol{v}[t]$ at sample times t_i with a sampling rate h. When measures are affected with noise values $\{\delta\boldsymbol{\eta}_{t_n}, \delta\boldsymbol{v}_{t_n}\}$, we use $\{\boldsymbol{\eta}_\delta[t_i], \boldsymbol{v}_\delta[t_i]\} = \left\{\boldsymbol{\eta}_{\delta_{t_i}}, \boldsymbol{v}_{\delta_{t_i}}\right\} = \{\boldsymbol{\eta}_{t_n} + \delta\boldsymbol{\eta}_{t_n}, \boldsymbol{v}_{t_n} + \delta\boldsymbol{v}_{t_n}\}$ instead.

Since the pure delay period is supposed to be originated in the control communication system, we will assume in some particular scenarios that T_d in (1), satisfies

$$T_d = d\ h = d_0\ h + \delta d\ h, \tag{3}$$

which is saying that d is a variable integer, while d_0 is a constant positive integer and δd a sign-undefined integer representing a perturbation that fulfills $d_0 \geq |\delta d| \geq 0$ and d can range between 0 and $2d_0$. Another feature of the communication hardware is that the sample times t_i of the instrument (from Gyro and DVL for instance) are indicated together with the samples, and so, when these are transmitted to the controller, the calculation of d is possible.

Now, let us rewrite the ODE (1)-(2) in a more compact form

$$\dot{\boldsymbol{v}} = M^{-1}\boldsymbol{p}[\boldsymbol{\eta}, \boldsymbol{v}] + M^{-1}\boldsymbol{\tau} \tag{4}$$

$$\dot{\boldsymbol{\eta}} = \boldsymbol{q}[\boldsymbol{\eta}, \boldsymbol{v}], \tag{5}$$

with $\boldsymbol{p}$ and $\boldsymbol{q}$ being Lipschitz vector functions located at the right-hand memberships of the (1) and (2), respectively. Here no exogenous perturbation was considered as agreed above.

For further analysis, we can state a model-based predictor for one step or more steps ahead. To this end it might employ high order approximators like Adams-Bashforth types, though for perturbed states a simple Euler approximator is more convenient (Jordán and Bustamante, 2009b). So

$$\boldsymbol{v}_{n+1} = \boldsymbol{v}_{t_n} + \delta\boldsymbol{v}_{t_n} + hM^{-1}\left(\boldsymbol{p}_{\delta_{t_n}} + \boldsymbol{\tau}_{n-d}\right) \tag{6}$$

$$\boldsymbol{\eta}_{n+1} = \boldsymbol{\eta}_{t_n} + \delta\boldsymbol{\eta}_{t_n} + h\boldsymbol{q}_{\delta_{t_n}}, \tag{7}$$

where $\boldsymbol{\eta}_{n+1}$ and $\boldsymbol{v}_{n+1}$ are one-step-ahead predictions. Herein it is valid with (1)-(2)

$$\boldsymbol{p}_{\delta_{t_n}} = -\sum_{i=1}^{6} C_i . \times C_{v_{i_n}} \boldsymbol{v}_{\delta_{t_n}} - D_l \boldsymbol{v}_{\delta_{t_n}} - \sum_{i=1}^{6} D_{q_i} \, |v_{i\delta_{t_n}}| \boldsymbol{v}_{\delta_{t_n}} - B_1 \, \boldsymbol{g}_{1_n} - B_2 \, \boldsymbol{g}_{2_n} \tag{8}$$

$$\boldsymbol{q}_{\delta_{t_n}} = J_{\delta_{t_n}} \boldsymbol{v}_{\delta_{t_n}} \tag{9}$$

where $C_{v_{i_n}}$ means $C_{v_i}[\boldsymbol{v}_{\delta_{t_n}}]$, $\boldsymbol{g}_{1_n}$ and $\boldsymbol{g}_{2_n}$ mean $\boldsymbol{g}_1[\boldsymbol{\eta}_{\delta_{t_n}}]$ and $\boldsymbol{g}_2[\boldsymbol{\eta}_{\delta_{t_n}}]$ respectively, $J_{\delta_{t_n}}$ means $J[\boldsymbol{\eta}_{\delta_{t_n}}]$ and $v_{i_{t_n}}$ is an element of $\boldsymbol{v}_{t_n}$. Additionally, the matricial product ".×" in (8) means an element-by-element product between the matrices to both sides. Besides, the control action $\boldsymbol{\tau}$ is retained one sampling period h by a sample holder, so it is valid $\boldsymbol{\tau}_n = \boldsymbol{\tau}_{t_n}$. We finally remark that since $\boldsymbol{p}$, $\boldsymbol{q}$ and $\boldsymbol{r}$ are Lipschitz continuous in the attraction domains in $\boldsymbol{v}$ and $\boldsymbol{\eta}$, then the samples, predictions and local errors all yield bounded.

4. Predictions

The accuracy of one-step-ahead predictions (6)-(7) with known perfect model and without perturbation is defined by the local model errors as

$$\boldsymbol{\varepsilon}_{v_{n+1}} = \boldsymbol{v}_{\delta_{t_{n+1}}} - \boldsymbol{v}_{n+1} \tag{10}$$

$$\boldsymbol{\varepsilon}_{\eta_{n+1}} = \boldsymbol{\eta}_{\delta_{t_{n+1}}} - \boldsymbol{\eta}_{n+1}. \tag{11}$$

with $\boldsymbol{\varepsilon}_{\eta_{n+1}}, \boldsymbol{\varepsilon}_{v_{n+1}} \in \mathcal{O}[h]$ and $\mathcal{O}$ being such a function that $f[x] \in \mathcal{O}[x]$ means that there exists a neighborhood of x around null such that $f[x]/x$ is bounded inside the neighborhood.

We have also the goal to predict states counteracting the negative influence of a delay in them. In order to be able to produce a prediction of many steps in advance based upon the last past information known, we can employ (6)-(7) tied in succession in many links of first order.

So we attempt to construct the state predictions $\boldsymbol{\eta}_{n+1}$ and $\boldsymbol{v}_{n+1}$ taken the sample at t_{n-d} as the unique support to predict at t_n. We start with

$$\boldsymbol{v}_{n-d+1} = \boldsymbol{v}_{\delta_{t_{n-d}}} + h\underline{M}^{-1} \left(\boldsymbol{r}_{\delta_{n-d}} + \boldsymbol{\tau}_{n-d} \right), \tag{12}$$

where $\boldsymbol{v}_{\delta_{t_{n-d}}}$ is the last sample known at the current time, $\underline{M}$ is some known lower matrix of M and

$$\boldsymbol{r}_j = \sum_{i=1}^{6} U_i . \times C_{v_{i_j}} \boldsymbol{v}_j + U_7 \boldsymbol{v}_j + \sum_{i=1}^{6} U_{7+i} |v_{i_j}| \boldsymbol{v}_j + U_{14} \boldsymbol{g}_{1_j} + U_{15} \, \boldsymbol{g}_{2_j}, \tag{13}$$

where the matrices U_i will account for every unknown system matrix in $\boldsymbol{p}_{\delta_{t_n}}$ in (8) with some appropriate value. We will return to these matrices U_i´s later in the controller design.

As there is no information of the sample at t_{n-d+1}, the next prediction is with (12) included

$$\boldsymbol{v}_{n-d+2} = \boldsymbol{v}_{\delta_{t_{n-d}}} + h\underline{M}^{-1} \left(\boldsymbol{r}_{n-d+1} + \boldsymbol{\tau}_{n-d+1} \right) + h\underline{M}^{-1} \left(\boldsymbol{r}_{\delta_{n-d}} + \boldsymbol{\tau}_{n-d} \right). \tag{14}$$

It is noticing the difference between $\boldsymbol{r}_{\delta_{n-d}}$ and $\boldsymbol{r}_{n-d+1}$ from the procedence of their variables, namely $\boldsymbol{r}_{\delta_{n-d}}$ is based upon the samples $\boldsymbol{v}_{\delta_{n-d}}$ and $\boldsymbol{\eta}_{\delta_{n-d}}$, while $\boldsymbol{r}_{n-d+1}$ is based upon the predictions $\boldsymbol{v}_{n-d+1}$ and $\boldsymbol{\eta}_{n-d+1}$.

For control purposes, the prediction for t_{n+1} will be necessary. This is

$$\boldsymbol{v}_{n+1} = \boldsymbol{v}_{\delta_{t_{n-d}}} + h\underline{M}^{-1} \sum_{i=1}^{d} (\boldsymbol{r}_{n+1-i} + \boldsymbol{\tau}_{n+1-i}) + h\underline{M}^{-1} \left(\boldsymbol{r}_{\delta_{n-d}} + \boldsymbol{\tau}_{n-d}\right), \tag{15}$$

$$\boldsymbol{\eta}_{n+1} = \boldsymbol{\eta}_{\delta_{t_{n-d}}} + h \sum_{i=1}^{d} \boldsymbol{q}_{n+1-i} + h\boldsymbol{q}_{\delta_{n-d}}. \tag{16}$$

The same consideration between $\boldsymbol{q}_{\delta_{n-d}}$ and $\boldsymbol{q}_{n-d+i}$ (for $i > 0$) mentioned before can be said as in the comparison made between $\boldsymbol{r}_{\delta_{n-d}}$ and $\boldsymbol{r}_{n-d+i}$ (for $i > 0$) with respect to samples and predictions.

As the so-called local truncation error of the Euler method is bounded, it is for $\boldsymbol{v}$

$$\alpha_0(h, \delta\boldsymbol{\eta}_{t_i}, \delta\boldsymbol{v}_{t_i}) = \max_{t_i > 0} \left| \frac{\boldsymbol{v}_{\delta_{t_i}} - \boldsymbol{v}_{i+1}}{h} - \underline{M}^{-1} \left(\boldsymbol{r}_{\delta_i} + \boldsymbol{\tau}_i\right) \right|, \tag{17}$$

and since the Method is consistent, $\alpha_0(h, \mathbf{0}, \mathbf{0})$ goes to zero as h tends to zero, then global error $\boldsymbol{\varepsilon}_{v_{n+1}}$ has a bound

$$|\boldsymbol{\varepsilon}_{v_{n+1}}| \le \left(\delta\boldsymbol{v}_{t_{n-d}} - \frac{\alpha_0(h, \delta\boldsymbol{\eta}_{t_i}, \delta\boldsymbol{v}_{t_i})}{\kappa_v} \right) e^{\kappa_v (\frac{T_d}{h} + 1)h}, \tag{18}$$

where κ_v is the Lipshitz constant of $\underline{M}^{-1} \left(\boldsymbol{p}[\boldsymbol{\eta}, \boldsymbol{v}] + \boldsymbol{\tau}\right)$. The same is said for $\boldsymbol{\eta}$, where there exists a Lipshitz constant κ_η of $\boldsymbol{q}[\boldsymbol{\eta}, \boldsymbol{v}]$ and it is valid

$$\left|\boldsymbol{\varepsilon}_{\eta_{n+1}}\right| \le \left(\delta\boldsymbol{\eta}_{t_{n-d}} - \frac{\beta_0(h, \delta\boldsymbol{\eta}_{t_i}, \delta\boldsymbol{v}_{t_i})}{\kappa_\eta} \right) e^{\kappa_\eta (\frac{T_d}{h} + 1)h}, \tag{19}$$

and

$$\beta_0(h, \delta\boldsymbol{\eta}_{t_i}, \delta\boldsymbol{v}_{t_i}) = \max_{t_i > 0} \left| \frac{\boldsymbol{\eta}_{\delta_{t_i}} - \boldsymbol{\eta}_{i+1}}{h} - \boldsymbol{q}_{\delta_i} \right|. \tag{20}$$

Clearly from (18) and (19), for any $T_d > 0$, the convergence of the predictions is ensured for h tending to zero and with $\delta\boldsymbol{\eta}$, $\delta\boldsymbol{v}$ uniformly null.

5. Design of the controller

Let the control system in Fig. 1 be taken as the basic structure for the next development. The guide system therein generates references in time, denoted by $\eta_r(t)$, of a geometric path in the 6-DOF with some desired kinematic, termed $v_r(\eta_r(t))$, over it. Additionally, it is assumed that the disturbances $\delta\eta_{t_n}$ and δv_{t_n} acting on the samples are uniformly bounded.

We now postulate a functional of the path error energy

$$Q_{t_n} = \breve{\eta}_{t_n}^T \breve{\eta}_{t_n} + \breve{v}_{t_n}^T \breve{v}_{t_n}, \tag{21}$$

with (see Jordán and Bustamante, 2011)

$$\breve{\eta}_{t_n} = \eta_{t_n} - \eta_{r_{t_n}} = \eta_n + \varepsilon_n - \eta_{r_{t_n}} \tag{22}$$

$$\breve{v}_{t_n} = v_{t_n} - J_{t_n}^{-1} \dot{\eta}_{r_{t_n}} + J_{t_n}^{-1} K_p \breve{\eta}_{t_n} = v_{t_n} + \varepsilon_{v_n} - J_{t_n}^{-1} \dot{\eta}_{r_{t_n}} + J_{t_n}^{-1} K_p \breve{\eta}_{t_n}, \tag{23}$$

where $K_p = K_p^T \geq 0$ is a design gain matrix affecting the geometric path errors. Clearly, if $\breve{\eta}_{t_n} \equiv \mathbf{0}$, then by (23) and (2), it yields $v_{t_n} - v_{r_{t_n}} \equiv \mathbf{0}$.

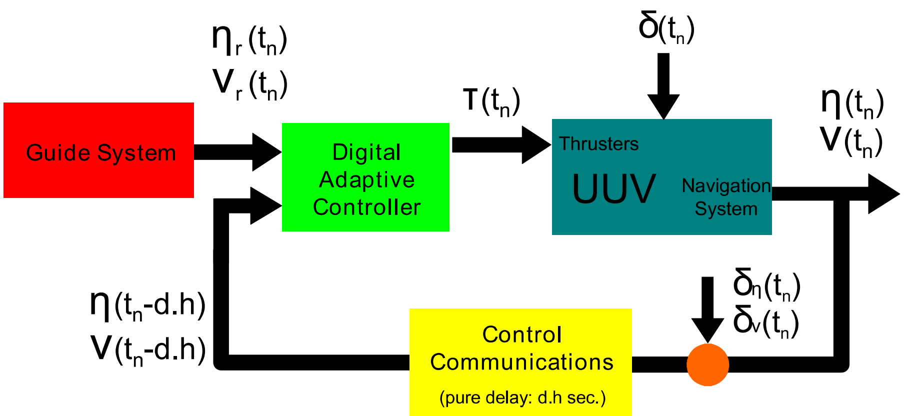

Figure 1. Digital adaptive control system of an UUV with sample disturbances and pure time delay in the control communication link

Then, replacing (6) and (7) in (22) for t_{n+1} one gets

$$\breve{\eta}_{t_{n+1}} = \eta_{n+1} + \varepsilon_{n+1} - \eta_{r_{t_{n+1}}} = \eta_n + hq_n + \varepsilon_n + \varepsilon_{n+1} - \eta_{r_{t_{n+1}}}. \tag{24}$$

Similarly, (6) and (7) in (23) for t_{n+1} one obtains

$$\begin{aligned} \breve{v}_{t_{n+1}} &= v_{t_{n+1}} - J_{t_{n+1}}^{-1} \dot{\eta}_{r_{t_{n+1}}} + J_{t_{n+1}}^{-1} K_p \breve{\eta}_{t_{n+1}} = \\ &= v_n + h\underline{M}^{-1} \left(r_{\delta_{n-d}} + \tau_{n-d} \right) + \varepsilon_{v_n} + \varepsilon_{v_{n+1}} - J_{t_{n+1}}^{-1} \dot{\eta}_{r_{t_{n+1}}} + J_{t_n+1}^{-1} K_p \breve{\eta}_{t_{n+1}}. \end{aligned} \tag{25}$$

http://dx.doi.org/10.5772/52224

The control goal is to construct the force τ_n so as to minimize Q_{t_n} asymptotically, with $\Delta Q_{t_n} := Q_{t_{n+1}} - Q_{t_n} < 0$

$$\Delta Q_{t_n} = \breve{\eta}^T_{t_{n+1}} \breve{\eta}_{t_{n+1}} + \breve{v}^T_{t_{n+1}} \breve{v}_{t_{n+1}} - \breve{\eta}^T_{t_n} \breve{\eta}_{t_n} - \breve{v}^T_{t_n} \breve{v}_{t_n}. \tag{26}$$

Bearing in mind the presence of disturbances and model uncertainties, the practical goal would be at least that $\{\Delta Q_{t_n}\}$ decrease so as to ultimately remain bounded for $t_n \to \infty$. The problem is now to construct the control action τ_n in such a way that this goal be achieved.

With (24), (25) and (21) in (26), one gets

$$\begin{aligned} \Delta Q_{t_n} = & \Big(\Big(I - hJ_{t_n} J_n^{-1} K_p \Big) \eta_n + hJ_{t_n} \breve{v}_{t_n} - hJ_{t_n} \varepsilon_{v_n} - hJ_{t_n} J_n^{-1} \dot{\eta}_{r_{t_n}} - \\ & - hJ_{t_n} J_n^{-1} K_p (\varepsilon_{\eta_n} - \eta_{r_{t_n}}) + \varepsilon_{\eta_n} + \varepsilon_{\eta_{n+1}} - \eta_{r_{t_{n+1}}} \Big)^2 - \\ & - \Big(\eta_n + \varepsilon_{\eta_n} - \eta_{r_{t_n}} \Big)^2 + \\ & + \Big(v_n + h\underline{M}^{-1} (r_n + \tau_n) + \varepsilon_{v_n} + \varepsilon_{v_{n+1}} - J_{t_{n+1}}^{-1} \dot{\eta}_{r_{t_{n+1}}} + J_{t_{n+1}}^{-1} K_p \breve{\eta}_{t_{n+1}} \Big)^2 - \\ & - \Big(v_n + \varepsilon_{v_n} - J_{t_{n+1}}^{-1} \dot{\eta}_{r_{t_n}} + J_{t_n}^{-1} K_p \breve{\eta}_{t_n} \Big)^2 . \end{aligned} \tag{27}$$

The desired properties of (27) can be conferred through a suitable selection of τ_n. In (Jordán and Bustamante, 2011) a flexible methodology for constructing τ_n was proposed and could serve to support this control objective. We will briefly review it and add the proper modifications attending the particularities of the pure-delay case.

Analyzing (27) we can conveniently split the control thrust τ_n into two terms as

$$\tau_n = \tau_{1_n} + \tau_{2_n}, \tag{28}$$

We notice that the choice

$$\tau_{1_n} = -K_v v_n - \frac{1}{h} \underline{M} \left(-J_{n+1}^{-1} \dot{\eta}_{r_{t_{n+1}}} + J_{n+1}^{-1} K_p \breve{\eta}_{n+1} \right) \tag{29}$$

is the most convenient to compensate some sign-undefinite terms in (27) and to propitiate a negative definite term in v_n. Herein $K_v = K_v^T \geq 0$ being another design matrix like K_p, but affecting the kinematic errors.

Thus

$$
\begin{aligned}
\Delta Q_{t_n} = {} & \left(\left(I - hJ_{t_n} J_n^{-1} K_p\right) \boldsymbol{\eta}_n\right)^2 - \boldsymbol{\eta}_n^2 + \left(\left(I - h\underline{M}^{-1} K_v\right) \boldsymbol{v}_n\right)^2 - \boldsymbol{v}_n^2 - \\
& - \left(J_{t_n}^{-1} \dot{\boldsymbol{\eta}}_{r_{t_n}} + J_{t_n}^{-1} K_p \breve{\boldsymbol{\eta}}_{t_n}\right)^2 - \boldsymbol{\eta}_{r_{t_n}}^2 + \left(-hJ_{t_n} \boldsymbol{\varepsilon}_{v_n} - hJ_{t_n} J_n^{-1} K_p \boldsymbol{\varepsilon}_{\eta_n} + \boldsymbol{\varepsilon}_{\eta_n} + \boldsymbol{\varepsilon}_{\eta_{n+1}}\right)^2 + \\
& + 2\boldsymbol{\varepsilon}_{\eta_n}^T \boldsymbol{\eta}_{r_{t_n}} - \boldsymbol{\varepsilon}_{\eta_n}^2 + \left(\boldsymbol{\varepsilon}_{v_n} + \boldsymbol{\varepsilon}_{v_{n+1}} - \Delta J_{n+1}^{-1} \dot{\boldsymbol{\eta}}_{r_{t_{n+1}}} + \Delta J_{n+1}^{-1} K_p \breve{\boldsymbol{\eta}}_{t_{n+1}}\right)^2 - \boldsymbol{\varepsilon}_{v_n}^2 + \\
& + 2\left(\left(I - hJ_{t_n} J_n^{-1} K_p\right) \boldsymbol{\eta}_n\right)^T \left(-hJ_{t_n} \boldsymbol{\varepsilon}_{v_n} - hJ_{t_n} J_n^{-1} K_p \boldsymbol{\varepsilon}_{\eta_n} + \right. \\
& \left. + \boldsymbol{\varepsilon}_{\eta_n} + \boldsymbol{\varepsilon}_{\eta_{n+1}}\right) - 2\boldsymbol{\eta}_n^T \left(\boldsymbol{\varepsilon}_{\eta_n} - \boldsymbol{\eta}_{r_{t_n}}\right) + 2\left(\left(I - h\underline{M}^{-1} K_v\right) \boldsymbol{v}_n\right)^T \\
& \left(\boldsymbol{\varepsilon}_{v_n} + \boldsymbol{\varepsilon}_{v_{n+1}} - \Delta J_{n+1}^{-1} \dot{\boldsymbol{\eta}}_{r_{t_{n+1}}} + \Delta J_{n+1}^{-1} K_p \breve{\boldsymbol{\eta}}_{t_{n+1}}\right) + \\
& + \left(h\underline{M}^{-1} \left(\boldsymbol{p}_n - \boldsymbol{r}_n\right)\right)^T \left(\boldsymbol{\varepsilon}_{v_n} + \boldsymbol{\varepsilon}_{v_{n+1}} - \Delta J_{n+1}^{-1} \dot{\boldsymbol{\eta}}_{r_{t_{n+1}}} + \Delta J_{n+1}^{-1} K_p \breve{\boldsymbol{\eta}}_{t_{n+1}}\right) - \\
& - \boldsymbol{v}_n^T \boldsymbol{\varepsilon}_{v_n} + \left(hJ_{t_n} \breve{\boldsymbol{v}}_{t_n} + hJ_{t_n} J_n^{-1} \dot{\boldsymbol{\eta}}_{r_{t_n}} + hJ_{t_n} J_n^{-1} K_p \boldsymbol{\eta}_{r_{t_n}} - \boldsymbol{\eta}_{r_{t_{n+1}}}\right)^2 + \\
& + 2\left(\left(I - hJ_{t_n} J_n^{-1} K_p\right) \boldsymbol{\eta}_n\right)^T \left(hJ_{t_n} \breve{\boldsymbol{v}}_{t_n} + hJ_{t_n} J_n^{-1} \dot{\boldsymbol{\eta}}_{r_{t_n}} + hJ_{t_n} J_n^{-1} K_p \boldsymbol{\eta}_{r_{t_n}} - \boldsymbol{\eta}_{r_{t_{n+1}}}\right) + \\
& + \left(h\underline{M}^{-1} \left(\boldsymbol{p}_n - \boldsymbol{r}_n\right)\right)^2 + 2\left(\left(I - h\underline{M}^{-1} K_v\right) \boldsymbol{v}_n\right)^T h\underline{M}^{-1} \left(\boldsymbol{p}_n - \boldsymbol{r}_n\right) - \\
& - 2\boldsymbol{v}_n^T \left(-J_{t_n}^{-1} \dot{\boldsymbol{\eta}}_{r_{t_n}} + J_{t_n}^{-1} K_p \breve{\boldsymbol{\eta}}_{t_n}\right) + \left(h\underline{M}^{-1} \boldsymbol{\tau}_{n_2}\right)^2 + \\
& + 2\left(\boldsymbol{v}_n + h\underline{M}^{-1} \left(\boldsymbol{p}_n - \boldsymbol{r}_n\right) + \boldsymbol{\varepsilon}_{v_n} + \boldsymbol{\varepsilon}_{v_{n+1}} - \Delta J_{n+1}^{-1} \dot{\boldsymbol{\eta}}_{r_{t_{n+1}}} + \Delta J_{n+1}^{-1} K_p \breve{\boldsymbol{\eta}}_{t_{n+1}}\right)^T h\underline{M}^{-1} \boldsymbol{\tau}_{n_2}
\end{aligned}
\tag{30}
$$

where $\boldsymbol{p}_n$ is defined as in $\boldsymbol{p}_{\delta_{t_n}}$ but with predictions $\boldsymbol{v}_n$ and $\boldsymbol{\eta}_n$ instead of $\boldsymbol{v}_{t_n}$ and $\boldsymbol{\eta}_{t_n}$, respectively. Similarly J_n stays for $J[\boldsymbol{\eta}_n]$. Additionally $\Delta J_{n+1}^{-1} = J_{t_{n+1}}^{-1} - J_{n+1}^{-1}$.

Finally, as seen in (30), the unique remaining design variable is $\boldsymbol{\tau}_{n_2}$.

A glance into (30) let us identify sign-undefinite terms which can not be compensated with $\boldsymbol{\tau}_{n_2}$, precisely because they are functions of unknown global prediction errors $\boldsymbol{\varepsilon}_\eta$, $\boldsymbol{\varepsilon}_v$, and ΔJ. We can group them into the function

$$f_{\Delta Q_1}[\varepsilon_{\eta_n},\varepsilon_{v_n}] = \left(-hJ_{t_n}\varepsilon_{v_n} - hJ_{t_n}J_n^{-1}K_p\varepsilon_{\eta_n} + \varepsilon_{\eta_n} + \varepsilon_{\eta_{n+1}}\right)^2 + 2\varepsilon_{\eta_n}^T\eta_{r_{t_n}} - \varepsilon_{\eta_n}^2 + \tag{31}$$
$$+ \left(\varepsilon_{v_n} + \varepsilon_{v_{n+1}} - \Delta J_{n+1}^{-1}\dot{\eta}_{r_{t_{n+1}}} + \Delta J_{n+1}^{-1}K_p\breve{\eta}_{t_{n+1}}\right)^2 - \varepsilon_{v_n}^2 +$$
$$+2\left(\left(I - hJ_{t_n}J_n^{-1}K_p\right)\eta_n\right)^T\left(-hJ_{t_n}\varepsilon_{v_n} - hJ_{t_n}J_n^{-1}K_p\varepsilon_{\eta_n} +\right.$$
$$\left. +\varepsilon_{\eta_n} + \varepsilon_{\eta_{n+1}}\right) + 2\left(\left(I - h\underline{M}^{-1}K_v\right)v_n\right)^T$$
$$\left(\varepsilon_{v_n} + \varepsilon_{v_{n+1}} - \Delta J_{n+1}^{-1}\dot{\eta}_{r_{t_{n+1}}} + \Delta J_{n+1}^{-1}K_p\breve{\eta}_{t_{n+1}}\right) +$$
$$+ \left(h\underline{M}^{-1}(p_n - r_n)\right)^T\left(\varepsilon_{v_n} + \varepsilon_{v_{n+1}} - \Delta J_{n+1}^{-1}\dot{\eta}_{r_{t_{n+1}}} + \Delta J_{n+1}^{-1}K_p\breve{\eta}_{t_{n+1}}\right) -$$
$$-v_n^T\varepsilon_{v_n} + 2\left(\varepsilon_{v_n} + \varepsilon_{v_{n+1}} - \Delta J_{n+1}^{-1}\dot{\eta}_{r_{t_{n+1}}} + \Delta J_{n+1}^{-1}K_p\breve{\eta}_{t_{n+1}}\right)^T h\underline{M}^{-1}\tau_{n_2}$$

which is consistent with ε_{η_n}, ε_{v_n}. So we have

$$\Delta Q_{t_n} = \left(\left(I - hJ_{t_n}J_n^{-1}K_p\right)\eta_n\right)^2 - \eta_n^2 + \left(\left(I - h\underline{M}^{-1}K_v\right)v_n\right)^2 - v_n^2 - \left(J_{t_n}^{-1}\dot{\eta}_{r_{t_n}} - J_{t_{n+1}}^{-1}K_p\breve{\eta}_{t_n}\right)^2 - \eta_{r_{t_n}}^2 +$$
$$+ f_{\Delta Q_1}[\varepsilon_{\eta_n},\varepsilon_{v_n}] + a\left(h\underline{M}^{-1}\tau_{n_2}\right)^2 + b_n^T\left(h\underline{M}^{-1}\tau_{n_2}\right) + c_n, \tag{32}$$

where the last three terms conform a complete quadratic polynomial in τ_{n_2} with coefficients

$$a = h^2 \tag{33}$$
$$b_n = 2h(I - hK_v^*)v_n + 2h\underline{M}^{-1}(p_n - r_n) \tag{34}$$
$$c_n = \left(hJ_{t_n}\breve{v}_{t_n} + hJ_{t_n}J_n^{-1}\dot{\eta}_{r_{t_n}} + hJ_{t_n}J_n^{-1}K_p\eta_{r_{t_n}} - \eta_{r_{t_{n+1}}}\right)^2 + \tag{35}$$
$$+2\left(\left(I - hJ_{t_n}J_n^{-1}K_p\right)\eta_n\right)^T\left(hJ_{t_n}\breve{v}_{t_n} + hJ_{t_n}J_n^{-1}\dot{\eta}_{r_{t_n}} + hJ_{t_n}J_n^{-1}K_p\eta_{r_{t_n}} - \eta_{r_{t_{n+1}}}\right) +$$
$$+ \left(h\underline{M}^{-1}(p_n - r_n)\right)^2 + 2\left(\left(I - h\underline{M}^{-1}K_v\right)v_n\right)^T h\underline{M}^{-1}(p_n - r_n) -$$
$$-2v_n^T\left(-J_{t_n}^{-1}\dot{\eta}_{r_{t_n}} + J_{t_n}^{-1}K_p\breve{\eta}_{t_n}\right),$$

with K_v^* being an auxiliary matrix equal to $K_v^* = M^{-1}K_v$.

Clearly, for eliminating these terms we need to implement one of the roots of the polynomial, it is

$$\tau_{2_n} = M\left(\frac{-b_n}{2a} \pm \frac{1}{2a}\sqrt{\frac{b_n^T b_n - 4ac_n}{6}}\mathbf{1}\right), \tag{36}$$

with **1** a vector with all elements equal one. However, there are some variables and parameters in these coefficients that are not known. So we can approximate them to

$$\bar{a} = h^2 \tag{37}$$

$$\overline{\boldsymbol{b}}_n = 2h(I - hK_v^*)\boldsymbol{v}_n \tag{38}$$

$$\begin{aligned}\bar{c}_n = &\left(hJ_n\breve{\boldsymbol{v}}_n + h\dot{\boldsymbol{\eta}}_{r_{t_n}} + hK_p\boldsymbol{\eta}_{r_{t_n}} - \boldsymbol{\eta}_{r_{t_{n+1}}}\right)^2 + \\ &+2\left(\left(I - hK_p\right)\boldsymbol{\eta}_n\right)^T\left(hJ_n\breve{\boldsymbol{v}}_n + h\dot{\boldsymbol{\eta}}_{r_{t_n}} + hK_p\boldsymbol{\eta}_{r_{t_n}} - \boldsymbol{\eta}_{r_{t_{n+1}}}\right) + \\ &-2\boldsymbol{v}_n^T\left(-J_n^{-1}\dot{\boldsymbol{\eta}}_{r_{t_n}} + J_n^{-1}K_p\breve{\boldsymbol{\eta}}_n\right).\end{aligned} \tag{39}$$

Finally we get the second component of $\boldsymbol{\tau}_n$ in an implementable way

$$\boldsymbol{\tau}_{2_n} = \underline{M}\left(\frac{-\overline{\boldsymbol{b}}_n}{2\bar{a}} \pm \frac{1}{2\bar{a}}\sqrt{\frac{\overline{\boldsymbol{b}}_n^T\overline{\boldsymbol{b}}_n - 4\bar{a}\overline{c_n}}{6}}\mathbf{1}\right). \tag{40}$$

Introducing the expression of $\boldsymbol{\tau}_n$ the functional remains

$$\begin{aligned}\Delta Q_{t_n} = &\left(\left(I - hJ_{t_n}J_n^{-1}K_p\right)\boldsymbol{\eta}_n\right)^2 - \boldsymbol{\eta}_n^2 + \left(\left(I - h\underline{M}^{-1}K_v\right)\boldsymbol{v}_n\right)^2 - \boldsymbol{v}_n^2 - \left(J_{t_n}^{-1}\dot{\boldsymbol{\eta}}_{r_{t_n}} - J_{t_{n+1}}^{-1}K_p\breve{\boldsymbol{\eta}}_{t_n}\right)^2 - \boldsymbol{\eta}_{r_{t_n}}^2 + \\ &+ f_{\Delta Q_1}[\boldsymbol{\varepsilon}_{\eta_n}, \boldsymbol{\varepsilon}_{v_n}] + f_{\Delta Q_2}[\boldsymbol{\varepsilon}_{\eta_n}, \boldsymbol{\varepsilon}_{v_n}],\end{aligned} \tag{41}$$

where the new error $f_{\Delta Q_2}$ is

$$\begin{aligned}f_{\Delta Q_2}[\boldsymbol{\varepsilon}_{\eta_n}, \boldsymbol{\varepsilon}_{v_n}] &= h\left(\boldsymbol{b}_n - \overline{\boldsymbol{b}}_n\right)^T\left(\frac{-\overline{\boldsymbol{b}}_n}{2\bar{a}} \pm \frac{1}{2\bar{a}}\sqrt{\frac{\overline{\boldsymbol{b}}^T\overline{\boldsymbol{b}} - 4\bar{a}\bar{c}}{6}}\mathbf{1}\right) + (c_n - \bar{c}_n) = \\ = &\frac{\underline{M}^{-1}(\boldsymbol{p}_n - \boldsymbol{r}_n)^T\left(2h(I - hK_v^*)\boldsymbol{v}_n + 2h\underline{M}^{-1}(\boldsymbol{p}_n - \boldsymbol{r}_n)\right)}{2h} + \\ &+ \frac{\underline{M}^{-1}(\boldsymbol{p}_n - \boldsymbol{r}_n)^T}{2h}\sqrt{\frac{\overline{\boldsymbol{b}}^T\overline{\boldsymbol{b}} - 4\bar{a}\bar{c}}{6}}\mathbf{1} + (c_n - \bar{c}_n).\end{aligned} \tag{42}$$

The properties of the error functions $f_{\Delta Q_1}$ and $f_{\Delta Q_2}$ and their influence in the stability of the control system is analyzed later. Previous to this task, we will illustrate the way we generate the matrices U_i's so as to calculate the variables $\boldsymbol{r}_i$ in (13).

6. Adaptive laws

The adaptation of the control behaviour to the unknown vehicle dynamics occurs by the permanent actualization of the controller matrices U_i.

Let the following adaptive law be valid for $i = 1, ..., 15$

$$U_{i_{n+1}} \triangleq U_{i_n} - \Gamma_i \frac{\partial \Delta Q_{t_n}}{\partial U_i}, \tag{43}$$

with a gain matrix $\Gamma_i = \Gamma_i^T \geq 0$ and $\frac{\partial \Delta Q_{t_n}}{\partial U_{i_n}}$ being a gradient matrix for U_{i_n}.

First we can define an expression for the gradient matrix upon ΔQ_{t_n} in (30) but considering that M is known. This expression is referred to the ideal gradient matrix

$$\begin{aligned} \frac{\partial \Delta Q_{t_n}}{\partial U_i} &= -2h^2 M^{-T} \left(M^{-1} \boldsymbol{\tau}_{2_n} \right) \left(\frac{\partial \boldsymbol{r}_n}{\partial U_i} \right)^T - \\ &\quad -2h^2 M^{-T} M^{-1} (\boldsymbol{p}_n - \boldsymbol{r}_n) \left(\frac{\partial \boldsymbol{r}_n}{\partial U_i} \right)^T - \\ &\quad -2h M^{-T} (I - hK_v^*) \breve{\boldsymbol{v}}_n \left(\frac{\partial \boldsymbol{r}_n}{\partial U_i} \right)^T . \end{aligned} \tag{44}$$

Now, in order to be able to implement adaptive laws like (43) we have to replace the unknown M in (44) by its lower bound $\underline{M}$. In this way, we can generate implementable gradient matrices which will denote by $\frac{\partial \overline{\Delta Q}_{t_n}}{\partial U_i}$ with

$$\begin{aligned} \frac{\partial \overline{\Delta Q}_{t_n}}{\partial U_i} &= -2h^2 \underline{M}^{-T} \left(\underline{M}^{-1} \boldsymbol{\tau}_{2_n} \right) \left(\frac{\partial \boldsymbol{r}_n}{\partial U_i} \right)^T - \\ &\quad -2h^2 \underline{M}^{-T} \underline{M}^{-1} (\boldsymbol{p}_n - \boldsymbol{r}_n) \left(\frac{\partial \boldsymbol{r}_n}{\partial U_i} \right)^T - \\ &\quad -2h \underline{M}^{-T} (I - hK_v^*) \breve{\boldsymbol{v}}_n \left(\frac{\partial \boldsymbol{r}_n}{\partial U_i} \right)^T , \end{aligned} \tag{45}$$

and the property

$$\frac{\partial \overline{\Delta Q}_{t_n}}{\partial U_i} = \frac{\partial \Delta Q_{t_n}}{\partial U_i} + \Delta_{U_{i_n}}, \tag{46}$$

where

$$\Delta_{U_{i_n}} = \delta_{M^{-2}} A_{i_n} + \delta_{M^{-1}} B_{i_n}, \tag{47}$$

and $\delta_{M^{-2}} = \left(\underline{M}^{-T}\underline{M}^{-1} - M^{-T}M^{-1}\right) \geq 0$ and $\delta_{M^{-1}} = \left(\underline{M}^{-1} - M^{-1}\right) \geq 0$. Here A_{i_n} and B_{i_n} are sampled state functions obtained from (44) after extracting of the common factors $\delta_{M^{-2}}$ and $\delta_{M^{-1}}$, respectively.

It is worth noticing that ΔQ_{t_n} and $\overline{\Delta Q}_{t_n}$, satisfy convexity properties in the space of elements of the U_i's.

Moreover, with (46) in mind we can conclude for any pair of values of U_i, say $U_i^{'}$ and $U_i^{''}$, it is valid

$$\Delta Q_{t_n}(U_i^{'}) - \Delta Q_{t_n}(U_i^{''}) \leq \frac{\partial \Delta Q_{t_n}(U_i^{''})}{\partial U_i}\left(U_i^{'} - U_i^{''}\right) \leq \tag{48}$$

$$\leq \frac{\partial \overline{\Delta Q}_{t_n}(U_i^{''})}{\partial U_i}\left(U_i^{'} - U_i^{''}\right). \tag{49}$$

This feature will be useful in the next analysis.

In summary, the practical laws which conform the digital adaptive controller are

$$U_{i_{n+1}} \triangleq U_{i_n} - \Gamma_i \frac{\partial \overline{\Delta Q}_{t_n}}{\partial U_i}. \tag{50}$$

Finally, it is seen from (45) that also here the noisy measures $\boldsymbol{\eta}_{\delta_{t_n}}$ and $\boldsymbol{v}_{\delta_{t_n}}$ will propagate into the adaptive laws $\frac{\partial \overline{\Delta Q}_{t_n}}{\partial U_i}$.

7. Stability analysis

It is worth noticing that the two first terms in (41) can satisfy $\left(\left(I - hJ_{t_n}J_n^{-1}K_p\right)\boldsymbol{\eta}_n\right)^2 - \boldsymbol{\eta}_n^2 < 0$ by proper selection of K_p and the following two terms can fulfill $\left(\left(I - h\underline{M}^{-1}K_v\right)\boldsymbol{v}_n\right)^2 - \boldsymbol{v}_n^2 <$ 0 by proper selection of K_v and so the sign of ΔQ_{t_n} for any trajectories $\breve{\boldsymbol{\eta}}_{t_n}$ and $\breve{\boldsymbol{v}}_{t_n}$ and initial conditions of them would be depending of error functions $f_{\Delta Q_1}$ and $f_{\Delta Q_2}$ only.

According to (18) and (19), we can argue that $f_{\Delta Q_1}$ in (31) and $f_{\Delta Q_2}$ in (42) are consistent with $\boldsymbol{\varepsilon}_\eta$ and $\boldsymbol{\varepsilon}_v$, it is, in absence of disturbances, they go to zero for h tending to zero. On the other hand, by existing disturbances $\delta\boldsymbol{\eta}_{t_n}$ and $\delta\boldsymbol{v}_{t_n}$, and any value of h, the maximal global errors are proportional to the disturbances. Clearly, the more extensive the pure dead time T_d, the larger the magnitude of $f_{\Delta Q_1}$ and $f_{\Delta Q_2}$, and this dependence is exponential.

To focus the stability problem in more detail, let first the controller matrices U_i's to take the values U_i^{*}'s. So, using these constant system matrices in (1), a fixed controller can be designed.

For this particular controller we consider the resulting $\Delta Q_{t_n}^{*}$ from (30) accomplishing

$$\Delta Q^{*}_{t_n}=\left(\left(I-hJ_{t_n}J_n^{-1}K_p\right)\boldsymbol{\eta}_n\right)^2-\boldsymbol{\eta}_n^2+\left(\left(I-h\underline{M}^{-1}K_v\right)\boldsymbol{v}_n\right)^2-\boldsymbol{v}_n^2-\left(J_{t_n}^{-1}\dot{\boldsymbol{\eta}}_{r_{t_n}}-J_{t_{n+1}}^{-1}K_p\breve{\boldsymbol{\eta}}_{t_n}\right)^2-\boldsymbol{\eta}_{r_{t_n}}^2+$$
$$+f^{*}_{\Delta Q}[\boldsymbol{\varepsilon}_{\eta_n},\boldsymbol{\varepsilon}_{v_n}\delta\boldsymbol{\eta}_{t_n},\delta\boldsymbol{v}_{t_n},M^{-1}\underline{M}], \tag{51}$$

where $f^{*}_{\Delta Q_n}$ is the sum of $f_{\Delta Q_1}$ and $f_{\Delta Q_2}$ obtained from (31) and (42), but with the condition $\boldsymbol{p}_n=\boldsymbol{r}_n$

$$f^{*}_{\Delta Q_n}\ = f_{\Delta Q_{1_n}}[\boldsymbol{p}_n=\boldsymbol{r}_n]+f_{\Delta Q_{2_n}}[\boldsymbol{p}_n=\boldsymbol{r}_n]. \tag{52}$$

Later, a norm of $f^{*}_{\Delta Q_n}$ will be indicated.

Since $\boldsymbol{\varepsilon}_{\eta_{n+1}}$, $\boldsymbol{\varepsilon}_{v_{n+1}}$, $\delta\boldsymbol{\eta}$, $\delta\boldsymbol{v}\in l_\infty$. Additionally, $M^{-1}\underline{M}$ is bounded. Thus, one concludes $f^{*}_{\Delta Q_n}\in l_\infty$ as well.

So, it is noticing that $\Delta Q^{*}_{t_n}<0$, at least in an attraction domain equal to

$$\mathcal{B}=\left\{\breve{\boldsymbol{\eta}}_{t_n},\breve{\boldsymbol{v}}_{t_n}\in\mathcal{R}^6\cap\mathcal{B}^*_0\right\}, \tag{53}$$

with $\mathcal{B}^*_0$ a residual set around zero

$$\mathcal{B}^*_0=\left\{\breve{\boldsymbol{\eta}}_{t_n},\breve{\boldsymbol{v}}_{t_n}\in\mathcal{R}^6/\Delta Q^{*}_{t_n}-f^{*}_{\Delta Q_n}\leq 0\right\} \tag{54}$$

and with the design matrices satisfying the conditions

$$2\frac{J_nJ_{t_n}^{-1}}{h}>K_p>0 \tag{55}$$
$$\frac{2}{h}I>K^*_v\geq 0, \tag{56}$$

which is equivalent to

$$\frac{2}{h}M\geq\frac{2}{h}\underline{M}>K_v\geq 0. \tag{57}$$

The residual set $\mathcal{B}^*_0$ depends not only on $\boldsymbol{\varepsilon}_{\eta_{n+1}}$ and $\boldsymbol{\varepsilon}_{v_{n+1}}$ and the measure noises $\delta\boldsymbol{\eta}_{t_n}$ and $\delta\boldsymbol{v}_{t_n}$, but also on $M^{-1}\underline{M}$. In consequence, $\mathcal{B}^*_0$ becomes the null point at the limit when $h\to 0$, $\delta\boldsymbol{\eta}_{t_n}$, $\delta\boldsymbol{v}_{t_n}\to 0$ and $\underline{M}=M$.

7.1. Stability proof

The problem of stability of the adaptive control system is addressed in the sequel. Let a Lyapunov function be

$$V_{t_n} = Q_{t_n} + \frac{1}{2}\sum_{i=1}^{15}\sum_{j=1}^{6}\left(\tilde{\boldsymbol{u}}_j^T\right)_{i_{n+1}} \Gamma_i^{-1}\left(\tilde{\boldsymbol{u}}_j\right)_{i_{n+1}} - \\ -\frac{1}{2}\sum_{i=1}^{15}\sum_{j=1}^{6}\left(\tilde{\boldsymbol{u}}_j^T\right)_{i_n} \Gamma_i^{-1}\left(\tilde{\boldsymbol{u}}_j\right)_{i_n}, \tag{58}$$

with $\left(\tilde{\boldsymbol{u}}_j\right)_{i_n} = \left(\boldsymbol{u}_j - \boldsymbol{u}_j^*\right)_{i_n}$, where $\boldsymbol{u}_j$ and $\boldsymbol{u}_j^*$ are vectors corresponding to the column j of the adaptive controller matrix U_i and its corresponding one U_i^* in the fixed controller, respectively. Then the differences $\Delta V_{t_n} = V_{t_{n+1}} - V_{t_n}$ can be bounded as follows

$$\begin{aligned}\Delta V_{t_n} &= \Delta Q_{t_n} + \frac{1}{2}\sum_{i=1}^{15}\sum_{j=1}^{6}\left(\Delta \boldsymbol{u}_j^T\right)_{i_n} \Gamma_i^{-1}\left(\left(\tilde{\boldsymbol{u}}_j\right)_{i_{n+1}} + \left(\tilde{\boldsymbol{u}}_j\right)_{i_n}\right) \\ &= \Delta Q_{t_n} + \sum_{i=1}^{15}\sum_{j=1}^{6}\left(\Delta \boldsymbol{u}_j^T\right)_{i_n} \Gamma_i^{-1}\left(\tilde{\boldsymbol{u}}_j\right)_{i_n} - \\ &-\frac{1}{2}\sum_{i=1}^{15}\sum_{j=1}^{6}\left(\Delta \boldsymbol{u}_j^T\right)_{i_n} \Gamma_i^{-1}\left(\Delta \boldsymbol{u}_j\right)_{i_n} \\ &\le \Delta Q_{t_n} - \sum_{i=1}^{15}\sum_{j=1}^{6}\left(\frac{\partial \Delta Q_{t_n}}{\partial \boldsymbol{u}_j}\right)^T \left(\tilde{\boldsymbol{u}}_j\right)_{i_n} \\ &\le \Delta Q_{t_n} - \sum_{i=1}^{15}\sum_{j=1}^{6}\left(\frac{\partial \overline{\Delta Q}_{t_n}}{\partial \boldsymbol{u}_j}\right)^T \left(\tilde{\boldsymbol{u}}_j\right)_{i_n} \\ &\le \Delta Q_{t_n}^* < 0 \text{ in } \mathcal{B} \cap \mathcal{B}_0^*,\end{aligned} \tag{59}$$

with $\left(\Delta \boldsymbol{u}_j\right)_{i_n}$ a column vector of $\left(U_{i_{n+1}} - U_{i_n}\right)$.

The column vector $\left(\Delta \boldsymbol{u}_j\right)_{i_n}$ at the first inequality was replaced by the column vector $-\Gamma_i\left(\frac{\partial \Delta Q_{t_n}}{\partial \boldsymbol{u}_j}\right)$ and then by $-\Gamma_i\left(\frac{\partial \overline{\Delta Q}_{t_n}}{\partial \boldsymbol{u}_j}\right)$ in the right member according to (46) and (48)-(49). So in the second and third inequality, the convexity property of ΔQ_{t_n} in (48) was applied for any pair $\left(U' = U_{i_n}, U'' = U_i^*\right)$.

This analysis has proved convergence of the error paths when real square root exist from $\sqrt{\overline{\boldsymbol{b}}_n^T \overline{\boldsymbol{b}}_n - 4\bar{a}\bar{c}_n}$ of (40).

http://dx.doi.org/10.5772/52224

If on the contrary $4\bar{a}\bar{c}_n > \overline{\boldsymbol{b}}_n^T\overline{\boldsymbol{b}}_n$ occurs at some time t_n, one chooses the real part of the complex roots in (40). So a suboptimal control action is employed instead equal to

$$\boldsymbol{\tau}_{2_n} = \frac{-1}{2\bar{a}}\underline{M}^{-1}\overline{\boldsymbol{b}}_n = \frac{-\underline{M}^{-1}}{h}(I - hK_v^*)\breve{\boldsymbol{v}}_{t_n}, \tag{60}$$

and yields a new functional $\Delta Q_{t_n}^{**}$ in

$$\Delta V_{t_n} \leq \Delta Q_{t_n}^{**} = \Delta Q_{t_n}^{*} + \bar{c}_n - \frac{1}{4h^2}\overline{\boldsymbol{b}}_n^T\overline{\boldsymbol{b}}_n < 0 \text{ in } \mathcal{B} \cap \mathcal{B}_0^{**}, \tag{61}$$

where $\Delta Q_{t_n}^{*}$ is (51) with a real root of (40) and $\mathcal{B}_0^{**}$ is a new residual set. It is worth noticing that the positive quantity $\left(\bar{c}_n - \frac{1}{4h^2}\overline{\boldsymbol{b}}_n^T\overline{\boldsymbol{b}}_n\right)$ can be reduced by choosing h small. Nevertheless, $\mathcal{B}_0^{**}$ results larger than $\mathcal{B}_0^{*}$ in (59), since its dimension depends not only on $\boldsymbol{\varepsilon}_{\eta_{n+1}}$ and $\boldsymbol{\varepsilon}_{v_{n+1}}$ but also on the magnitude of $\left(\bar{c}_n - \frac{1}{4h^2}\overline{\boldsymbol{b}}_n^T\overline{\boldsymbol{b}}_n\right)$.

This closes the stability and convergence proof.

7.2. Variable boundness

With respect to the boundness of the adaptive matrices U_i´s it is seen from (45) that the gradients are bounded. Also the third term is more dominant than the remainder ones for h small ($h << 1$), and so, the kinematic error $\breve{\boldsymbol{v}}_{t_n}$ influences the intensity and sign of $\partial\overline{\Delta Q}_{t_n}/\partial U_i$ more significantly than the others. From (43) one concludes than the increasing of $|U_i|$ may not be avoided long term, however some robust modification techniques like a projection zone can be employed to achieve boundness. This is not developed here. The author can consult for instance (Ioannou and Sun, 1996).

7.3. Instability for large sampling time and pure delay

Broadly speaking, the influence of the analyzed parameters will play a role in the instability when the chosen h is something large, even smaller than one, because the quadratic terms rise a turn off dominant in the error function $f_{\Delta Q_n}^*$.

The study of this phenomenon is rather complex. It involves the function $\Delta Q_{t_n}^{*}$ in (51) and $f_{\Delta Q_n}^*$ in (52).

Qualitatively speaking, when

$$f_{\Delta Q_n}^* < -\left(\left(I - hJ_{t_n}J_n^{-1}K_p\right)\boldsymbol{\eta}_n\right)^2 + \boldsymbol{\eta}_n^2 - \left(\left(I - h\underline{M}^{-1}K_v\right)\boldsymbol{v}_n\right)^2 + \boldsymbol{v}_n^2 + \left(J_{t_n}^{-1}\dot{\boldsymbol{\eta}}_{r_{t_n}} - J_{t_{n+1}}^{-1}K_p\breve{\boldsymbol{\eta}}_{t_n}\right)^2 + \boldsymbol{\eta}_{r_{t_n}}^2, \tag{62}$$

the path trajectories may not be bounded into a residual set because the domain for the initial conditions in this situation is partially repulsive. So, depending on the particular initial conditions and for $h >> 0$, or similarly for T_d large, the adaptive control system may turn unstable.

In conclusion, when comparing two digital controllers, the sensitivity of the stability to h and indirectly the presence of large pure delays in the dynamics, is fundamental to draw out robust properties and finally to range them.

8. Adaptive control algorithm

The adaptive control algorithm can be summarized as follows.

Preliminaries:

1) Estimate a lower bound $\underline{M}$, for instance $\underline{M} = M_b$ (Jordán & Bustamante, 2011),

2) Select a sampling time h as small as possible,

3) Choose design gain matrices K_p and K_v according to (56)-(57), and simultaneously in order to reduce $f^*_{\Delta Q_n}$ and $\Delta Q^*_{t_n}$ (see related commentary in previous section),

4) Define the adaptive gain matrices Γ_i (usually $\Gamma_i = \alpha_i I$ with $\alpha_i > 0$),

5) Stipulate the desired sampled-data path references for the geometric and kinematic trajectories in 6 DOF´s: $\boldsymbol{\eta}_{r_{t_n}}$ and $\boldsymbol{v}_{r_{t_n}}$, respectively (see related commentary in previous section),

Continuously at each sample point:

6) Calculate the control thrust $\boldsymbol{\tau}_n$ with components $\boldsymbol{\tau}_{1_n}$in (29) and $\boldsymbol{\tau}_{2_n}$ (40) (or (60)), respectively,

7) Calculate the adaptive controller matrices (44) with the lower bound $\underline{M}$ instead of M,

Long-term tuning:

7) Redefine K_p, K_v and h in order to achieve optimal tracking performance.

Remark

For the present approach, we can summarize the different steps carried out in this Chapter after the control design in order to determine its convergence properties and performance of the control system:

a) Establishment of the adaptive laws for the designed controller using a lower bound of M (Section 6),

b) Stability and convergence analysis of the control system to a residual set dependent of the sign-undefinite terms $f_{\Delta Q_1}$ and $f_{\Delta Q_2}$ in (31) and (42), respectively, which depend on the pure dead-time T_d (Section 7). Moreover, the conjoint incidence of local model errors $\boldsymbol{\varepsilon}_{\eta_{n+1}}$ and $\boldsymbol{\varepsilon}_{v_{n+1}}$, measure noises $\delta\boldsymbol{\eta}_{t_n}$ and $\delta\boldsymbol{v}_{t_n}$, and the product $M^{-1}\underline{M}$ in the the convergence of state trajectories to a residual set $\mathcal{B}^*_0$ is illustrated in (Section 7.1).

http://dx.doi.org/10.5772/52224

c) Proof of boundness of the adaptive controller matrices U_i's and the way to ensure this (Section 7.2),

d) Analysis of a stability condition involving both huge sampling times and a large pure delays (Section 7.3).

9. Case study

With the end of illustrating the features of our control system approach, we simulate a path-tracking problem in 6 DOF´s for an underwater vehicle in a planar motion with some sporadic immersions to the floor.

A continuous-time model of a fully-maneuverable underwater vehicle is employed for the numerical simulations and a pure dead time in the control transmission was included. Details of this dynamics are given in (Jordán & Bustamante, 2009a).

We present the simulation of the adaptive control algorithm summarized in the previous section for an immersion in the depth (motion in the heave modus z) with translations aside in the modes surge x and sway y simultaneously.

Fig. 2 illustrates the evolution of the six controlled modes of the UUV in the descending. The initial conditions of the UUV at t_0 were $\boldsymbol{\eta}(0)=[1.1; 1.1; 1.1; 0.1; 0.1; 0.1]$ and $\boldsymbol{v}(0)=[0.1; 0.1; 0.1; 0.1; 0.1; 0.1]$. The design matrices were set in $K_p = K_v = I$. The sampling period was selected $h = 0.1$ s.

It is seen that after a short transient, which is not longer than 7 s, the UUV is positioned at the coordinates to the start point. Then it begins to the maneuver of descending. In the meantime the matrices U_i's are adapted and the path tracking result asymptotically convergent with unappreciated stationary errors. The predictors are sufficiently accurate during the evolution of the states.

In the simulation, between 20 s and 30 s, it can be seen a high interaction between the traslational modes which are tracked (namely: x, y, z) and the rotational modes which are regulated about zero only (namely: φ, θ, ψ). In the last ones, it one observes a significant variation of these magnitudes. However, this is reasonable considering the dynamics with large dead-times we are dealing with.

10. Conclusions

Often in complex digital control systems, for instance digital adaptive controllers in conjugation with complex dynamics with high degree of state interaction, the role played by the sampling time h is the algid point in the stability and control performance analysis. This is so because of the potential instability that may occur by improperly selected large h. This phenomenon is commonly magnified when a dead time is present. In any case, the appearance of perturbations and delays together in the dynamics makes the problem difficult to seize and comprehend.

An important example which meets these particularities is found in the control problem represented by the guidance of UUV´s in 6 DOF´s, which was taken here as case study.

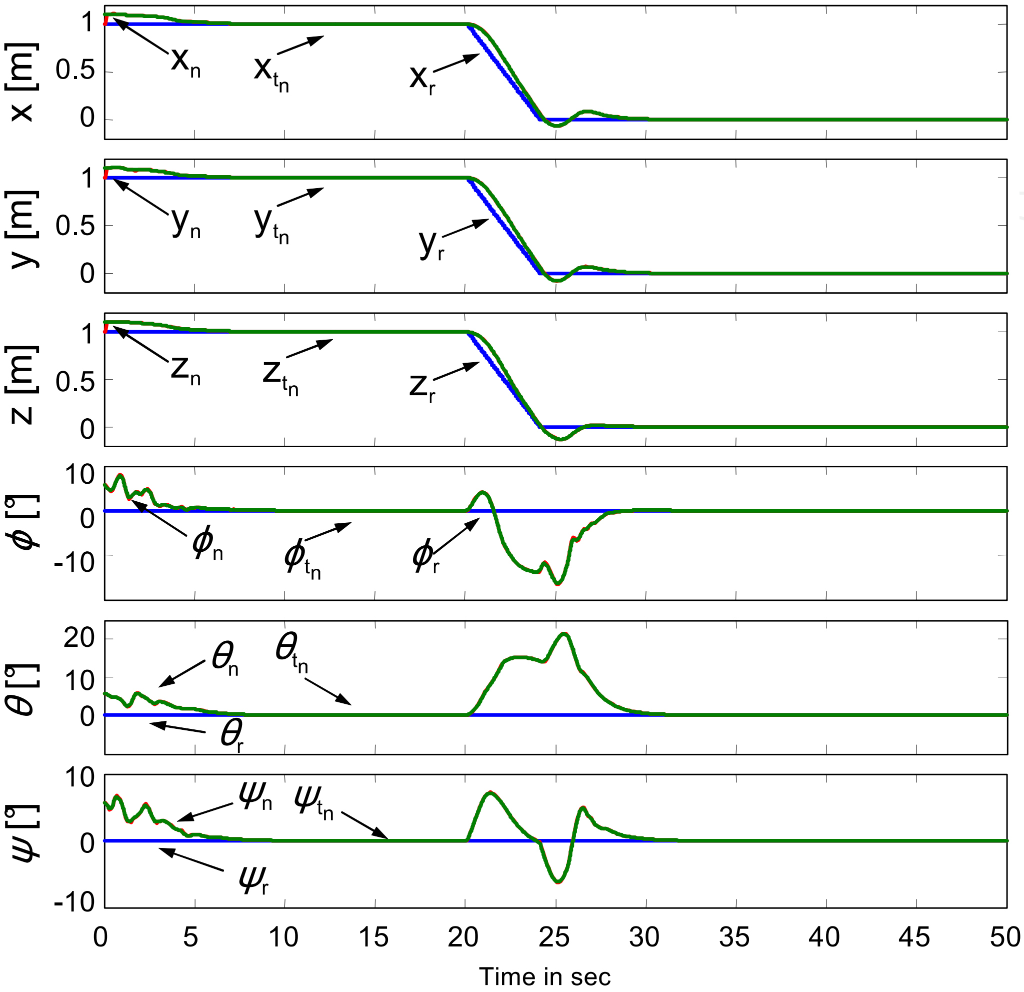

Figure 2. Evolution of the behaviour of a simulated UUV with adaptive control in all its modes.

Taking into consideration the hole of information caused by the presence of a pure delay in the adaptive control, we employs a filter for estimation of the actual state vector based on past measures together with a set of adaptive control matrices available over the delay period. The control end in the design is the minimization of certain incremental functional of the path energies of the geometric and kinematic errors. The control action can be then computed from predictions, as well as from the updating of the adaptive laws which succeeds with a support of filtered data at any discrete time.

We relate the stability and control performance with certain sign non-definite terms that are present in the final incremental functional of energy. From therein it can be concluded about the existence of an attraction domain and a residual set. This last one is influenced in size by the local errors of predictions, the perturbations δ in the measurements and the pure discrete delay d. It was clearly shown, that the presence of d does affect exponentially in magnitude the size of the prediction errors, which may be critical for the control stability if h is not selected sufficiently small.

Author details

Mario A. Jordan[1,2],
Jorge L. Bustamante[1,2] and Carlos E. Berger[1]

1 Instituto Argentino de Oceanografía IADO CCT-CONICET Bahía Blanca, Argentina
2 Universidad Nacional del Sur, Dto. de Ing. Eléctrica y de Computadoras UNS-DIEC, Bahía Blanca, Argentina

References

[1] Fossen, T.I. (1994). *Guidance and control of ocean vehicles*, John Wiley&Sons, New York, USA.

[2] Fradkov, A.L., Miroshnik, I.V. y Nikiforov, V.O. (1999), *Nonlinear and adaptive control of complex systems*, Kluwer Acad. Pub.

[3] Jordán, M.A. and J.L Bustamante (2007). On the presence of nonlinear oscillations in the teleoperation of underwater vehicles under the influence of sea, wave and current. In: *26th American Control Conference (2007 ACC)*. New York City, USA, July 11-13.

[4] Jordán, M.A. and J.L. Bustamante (2008). Guidance of underwater vehicles with cable tug perturbations under fixed and adaptive control modus. *IEEE J. of Oceanic Engineering*, 34(4), 579-598.

[5] Jordán, M.A. and J.L. Bustamante (2009a). *Adaptive Control for Guidance of Underwater Vehicles. In: Underwater Vehicles*, A.V. Inzartev (Editor), Chap. 14, 251-278. In-Tech, Vienna, Austria.

[6] Jordán, M.A. and J.L. Bustamante (2009b). Adams-Bashforth approximations for digital control of complex vehicle dynamics. In: *4th Int. Scientific Conf. on Physics and Control (PHYSCON 2009)*, Catania, Italy, Sep. 1-4.

[7] Jordán, M.A. and J.L. Bustamante (2011). *A General approach to discrete-time adaptive control systems with perturbed measures for complex dynamics. Case Study: unmanned underwater vehicles*. In: *Discrete Time Systems*. M.A. Jordán and J.B. Bustamante (Ed.). Chap. 15, 255-289. In-Tech, Rijeka, Croatia.

[8] Ioannou P. and J. Sun (1996). *Robust Adaptive Control,* Prentice Hall, New Jersey, USA.

[9] Leonard, F. and Abba, G. (2012). Robustness and Safe Sampling of Distributed-Delay Control Laws for Unstable Delayed Systems . *IEEE Transactions on Automatic Control*, 57 (6), 1521-1526.

IntechOpen